Journal of Systems Engineering and Electronics
Vol. 30, No. 3, June 2019, pp.587 – 600

Time-varying fault-tolerant formation tracking based cooperative control and guidance for multiple cruise missile systems under actuator failures and directed topologies

XU Xingguang[1,2], WEI Zhenyan[1,3,*], REN Zhang[1], and LI Shusheng[2]

1. School of Automation Science and Electrical Engineering, Beihang University, Beijing 100191, China;
2. Beijing Institute of Mechanical and Electrical Engineering, Beijing 100074, China;
3. Beijing Aerospace Technology Institute, Beijing 100074, China

Abstract: This paper studies time-varying fault-tolerant formation tracking problems for the multiple cruise missile system under directed topologies subjected to actuator failures. Firstly, the time-varying fault-tolerant formation tracking process for the multiple cruise missile system is divided into the guidance loop and the control loop. Then protocols are constructed to accomplish distributed fault-tolerant formation tracking in the guidance loop with the adaptive updating mechanism, in the condition where neither the knowledge about actuator malfunctions nor any global information of the communication topology remains available. Moreover, sufficient conditions to accomplish formation tracking are presented, and it is shown that the multiple cruise missile system can carry on the predefined time-varying fault-tolerant control (FTC) formation tracking through the active disturbances rejection controller (ADRC) and the proportion integration (PI) controller by the way of the fault-tolerant protocol utilizing the designed strategies, in the event of actuator failures. At last, numerical analysis and simulation are designed to verify the theoretical results.

Keywords: fault-tolerant, formation tracking, consensus-based, cruise missile, active disturbances rejection controller (ADRC).

DOI: 10.21629/JSEE.2019.03.16

1. Introduction

Recently, multiple cruise missile combat modes in the framework of the multi-agent system have been hot military and academic topics. Cooperative control and guidance of multi-agent systems play a critical role in the above-mentioned combat modes. As an important branch of cooperative control, formation control problems have been paid considerable attention from not only the tactical missiles aspect, but also different practical scenarios, such as autonomous underwater vehicles [1], spacecraft formation [2], unmanned aerial vehicles (UAVs) formation [3 – 5], mobile robots formation [6], etc. The aim of formation control is to allow the states of a flock of agents to maintain certain geometries eventually. It has been issues of common concern to investigate distributed formation control protocols utilizing one's neighborhood state information. Classic formation control approaches are mainly classified into behavior-based ones, virtual structure, and leader-follower, yet there exists downsides in these three strategies.

In the past few decades, the consensus-based formation control techniques have been researched extensively, and the above approaches can be translated into the consensus-based ones. Due to the universal nature of second-order systems in depicting the dynamic characteristics of the agent, [7 – 14] discussed distributed formation guidance and control questions for second-order swarm systems with directed connected topologies.

Currently, formation tracking problems, in which all the followers should follow up the state trajectory generated by the only leader while achieving desired formation configuration, have gained a lot of attention [15 – 21]. In [15], the formation tracking issue for the second-order swarm system with switching communication topologies was investigated, and these proposed approaches were extended to the practical application of target enclosing for a multi-quadrotor system. Dong et al. [16] proposed a time-varying formation tracking protocol in a totally distributed form for second-order multi-agent systems and addressed potential applications in multiple vehicles. Time-varying formation tracking measures were presented for the swarm system with more than one leader in [17]. [18,19] developed different formation tracking algorithms for second-order

Manuscript received August 23, 2018.
*Corresponding author.
This work was supported by the Natural Science Foundation of China (61101004; 61803014).

swarm systems utilizing neighboring information with or without velocity information respectively. Liu et al. [20] put forward impulsive control approaches to deal with formation tracking problems, where both followers and the leader were modeled as identical nonlinear oscillator.

It should be emphasized that, due to the complexity and uncertainty of dynamic characteristics, each agent for multi-agent systems may encounter actuator failures, and the malfunction may spread between adjacent agents through an interactive topology, which can cause disruptive failures throughout the system. It is well-known that in practical multiple cruise missile systems, elevators and engine failures may occur anytime and dramatically change the system's capability resulting in degradation or even instability (see e.g., [22 – 24] and the references therein). However, the actuator invalidation problems were not considered in [7 – 21].

Fault-tolerant control (FTC) is considered to be one of the best control methods for maintaining the good performance of each agent in the event of an unexpected failure. In view of these merits, it is of great significance to deal with FTC and guidance problems for the multiple cruise missile system in the event of actuator malfunctions. The FTC problem for multiple cruise missile systems which suffer from actuator failures was discussed in [25 – 31]. As far as we know, how to design time-varying FTC formation tracking protocols for multiple cruise missile systems under directed topologies in the event of actuator malfunctions is still open.

This paper discusses the time-varying FTC formation tracking control problem for the multiple cruise missile system subjected to actuator failures and directed topologies. Firstly, the formation tracking of the multiple cruise missile system is divided into the guidance loop and the control loop. The kinematic model of cruise missiles is simplified into a second-order system. Then a distributed formation tracking control measure is proposed in the guidance loop using the adaptive law, where information for actuator malfunctions is uncharted yet, and only the relative information for the adjacent agents is available. Moreover, formation tracking conditions are addressed, the validity of the proposed methods is verified to develop the formation tracking protocol, and the multi-agent system can realize time-varying formation tracking in the event of actuator failures. The above results are applied to the control loop, and the control strategy using the active disturbances rejection controller (ADRC) and the proportion integration (PI) controller are constructed by way of acceleration tracking. At last, the practical application of theoretical results in formation tracking control of the multiple cruise missile system is introduced.

Compared with related studies, the contributions of this paper are threefold. First of all, the fault-tolerant time-varying formation tracking problems of the multiple cruise missile systems are investigated, where the whole process is divided into the guidance loop and the control loop. The FTC strategy is taken into account in the guidance loop and achieved through the ADRC and the PI controller in the control loop. However, lots of previous studies about simultaneous attack of multiple missile mainly focus on the impact-time control guidance (ITCG) [32 – 35], and the practical application of fault-tolerant formation tracking approaches for turbojet engine driven cruise missiles has not been fully studied yet in relevant studies. Secondly, this paper gives time-varying fault-tolerant formation tracking problems in which there are a leader and numerous followers, instead of [15 – 21,25 – 31]. In [15 – 21], the failure problem of actuators is not taken into account when developing the time-varying formation tracking control protocol; furthermore, multi-agent systems cannot maintain the required performance when these protocols are applied directly in the event of actuator failure. In [25 – 31], the FTC strategies are put forward for swarm systems in the event of gain and bias actuator failures. However, in the design of the FTC strategy, only the formation problem without target enclosing is taken into account. Thirdly, an extended state observer (ESO) is utilized to estimate the unknown dynamics of the turbojet engine, and the coupling nonlinearities in the turbojet engine thrust modeling can be counteracted by the ADRC controller proposed in the control loop. The approaches for dealing with the cruise missile engine throttle control are seldom seen in the existing works.

The remainder of the paper is formulated as follows. Basic results and concept about graph theory and the horizontal mathematical model for cruise missiles are proposed, and the problem description is put forward in Section 2. Section 3 provides main results on the time-varying FTC formation tracking issues. The numerical simulation is presented in Section 4. Finally, this paper is concluded by Section 5.

2. Preliminaries and problem description

In this section, basic results and concepts on graph theory are introduced, then the horizontal mathematical model of the cruise missile and the problem description are presented.

2.1 Basic results and concepts on graph theory

The communication topology for swarm systems can be denoted by the directed graph $\boldsymbol{G} = \{\boldsymbol{V}, \boldsymbol{E}, \boldsymbol{W}\}$, where $\boldsymbol{E} \subseteq \{(v_k, v_j) : v_k, v_j \in \boldsymbol{V}, k \neq j\}$, $\boldsymbol{V} =$

$\{v_1, v_2, \ldots, v_N\}$, and $\boldsymbol{W} = [w_{kj}] \in \mathbf{R}^{N\times N}$ $(w_{kj} \geqslant 0)$ are called the edge set, the node set, and the weighted adjacency matrix in relation to the graph $\boldsymbol{G}$, separately. The edge is represented by $e_{kj} = (v_k, v_j)$ in $\boldsymbol{G}$. For any $k, j \in \{1, 2, \ldots, N\}$, $w_{jk} > 0$, if and only if $e_{kj} \in \boldsymbol{E}$; or $w_{jk} = 0$, otherwise. The neighbor set of the node v_k is defined as $\boldsymbol{N}_k = \{v_j \in \boldsymbol{V} : (v_j, v_k) \in \boldsymbol{E}\}$. The in-degree of the node k is represented by $\deg_{\text{in}}(v_k) = \sum_{j=1}^{N} w_{kj}$. Let $\boldsymbol{D} = \text{diag}\{\deg_{\text{in}}(v_k), k = 1, 2, \ldots, N\}$ be the degree matrix of $\boldsymbol{G}$. Furthermore, $\boldsymbol{L} = \boldsymbol{D} - \boldsymbol{W}$ describes the Laplacian matrix for the communication topology $\boldsymbol{G}$. Directed paths from the node v_k to the node v_j are a series of sequential edges with the form of $(v_{k_i}, v_{k_{i+l}})$, where $v_{k_i} \in \boldsymbol{V} (i = 1, \ldots, l-1)$. The directed graph is called to include a spanning tree if there is no fewer than one node containing a directed path to any other nodes.

The communication topology among the N agents can be represented by the graph $\boldsymbol{G}$ with each agent being a node in $\boldsymbol{G}$ and the communication interaction from the agent k $(k \in \{1, \ldots, N\})$ to the agent j $(j \in F)$ can be denoted by the edge e_{kj}. An agent is called a follower if it contains at least one neighbor and is said to be a leader if it has no neighbors. In this paper, cruise missiles are chosen as multiple followers, and the military attack target of the cruise missile system is denoted as the leader.

Lemma 1 [12] If the directed communication interaction topology $\boldsymbol{G}$ is connected, then (i) zero is a simple eigenvalue for the Laplacian matrix $\boldsymbol{L}$, whereas any other $N-1$ eigenvalues contain positive real parts; (ii) there is a non-negative vector $\boldsymbol{\varepsilon} = [\varepsilon_1, \varepsilon_2, \ldots, \varepsilon_N]^{\mathrm{T}}$ satisfying $\sum_{i=1}^{N} \varepsilon_i = 1$ and $\boldsymbol{\varepsilon}^{\mathrm{T}}\boldsymbol{L} = 0$; (iii) let $\boldsymbol{\Gamma} = \text{diag}\{\varepsilon_1, \varepsilon_2, \ldots, \varepsilon_N\}$, and therefore $\widehat{\boldsymbol{L}} = \boldsymbol{\Gamma}\boldsymbol{L} + \boldsymbol{L}^{\mathrm{T}}\boldsymbol{\Gamma}$ is a symmetric Laplacian matrix in relation to an connected undirected communication topology. Furthermore, let $\boldsymbol{\upsilon} \in \mathbf{R}^{N\times 1}$ stand for any non-negative column vectors and $\lambda_2(\widehat{\boldsymbol{L}})$ specifies the minimum non-zero eigenvalue for the Laplacian matrix $\widehat{\boldsymbol{L}}$. For $\boldsymbol{\mu}(t) \in \mathbf{R}^{N\times 1}$, it holds that

$$\min_{\boldsymbol{\mu}^{\mathrm{T}}(t)\boldsymbol{\nu}=0} \{\boldsymbol{\mu}^{\mathrm{T}}(t)\widehat{\boldsymbol{L}}\boldsymbol{\mu}(t)\} > \frac{\lambda_2(\widehat{\boldsymbol{L}})}{N}\boldsymbol{\mu}^{\mathrm{T}}(t)\boldsymbol{\mu}(t).$$

2.2 Cruise missile modeling

Multiple cruise missile systems are expected to perform formation tracking tasks in the horizontal $X-O-Z$ plane. The dynamic characteristics of cruise missiles can be classified into trajectory dynamics and attitude dynamics, where the time constant of the latter is much smaller than the time constant of the former. Therefore, we can make the following assumptions in this section.

Assumption 1 Cruise missiles fly at constant heights and the sideslip angle β is assumed to be zero. The effect of rotation and short period process is assumed to be ignored in the motion track formation.

Considering the horizontal dynamic characteristics model for the Tomahawk cruise missile, which is a tactical missile flying at subsonic speed with a single-engine unit developed by the convair division of the general dynamics corporation [36–39], Table 1 displays the needed model parameters.

Table 1 Tomahawk cruise missile parameters

Parameter	Value
Flight height/m	100
Flight speed/Ma	0.72
Mass/kg	1 315
Fuselage length/mm	5 560
Wingspan/mm	2 650
Engine thrust/kgf	267

In straight and level flight, the force balance and the instantaneous equilibrium can be achieved in the Y direction within the flight envelope (see Fig. 1). Based upon Assumption 1, acceleration in the Z direction can be rewritten in a form represented by the missile gravity $\boldsymbol{G}_m$.

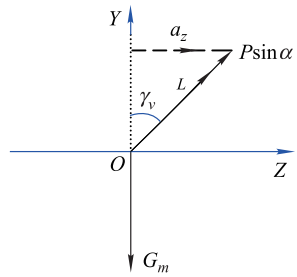

Fig. 1 Forces acting on the cruise missile in $\boldsymbol{Y-O-Z}$ plane

Then the horizontal mathematical model for cruise missiles can be described as

$$\begin{cases} \dot{v}_x = (P\cos\alpha - C_x qS)/m \\ \dot{v}_z = g\tan\gamma_v \\ (P\sin\alpha + C_y qS)\cos\gamma_v = mg \end{cases} \tag{1}$$

where v_x, v_z, α, m, γ_v, q, S and g denote acceleration along the X direction and the Z direction, the angle of attack, mass, the bank angle, the dynamic pressure, the reference area, and gravitational acceleration, respectively. P, C_x and C_y represent the turbojet engine thrust, the drag and the lift coefficients. Besides, the following conditions are satisfied:

$$\begin{cases} C_x = c_{x0} + c_x^{\alpha}\alpha^2 \\ C_y = c_y^{\alpha}\alpha \\ P = P(\phi) \end{cases}. \tag{2}$$

Note that P is relevant to the turbojet engine throttle setting ϕ, which can be denoted by the first-order linear equation with intrinsic nonlinear dynamics as

$$P = P_0 + P_1\phi + d(\phi) \tag{3}$$

where P_0 and P_1 are composition terms of the linear equation, and $d(\phi)$ is the bounded uncertain nonlinear function with $|d(\phi)| \leqslant D$ ($D \in \mathbf{R}^+$).

From (1) and (3), one can infer that acceleration tracking along the X direction together with the Z direction will be accomplished through regulating the speed bank angle and the turbojet engine throttle setting.

A over-damped second-order element is appended to the input ϕ of the turbojet engine, choosing the commanded value ϕ_C as the new input, that is

$$G_f(s) = \frac{\phi(s)}{\phi_C(s)} = \frac{\omega_n^2}{s^2 + 2\xi\omega_n s + \omega_n^2}, \quad \xi > 1. \tag{4}$$

2.3 Problem description

The formation tracking for the multiple cruise missile system is required to be divided into two sub-processes, that is, the guidance loop and the control loop. For the sake of maintaining the desired formation tracking performance of the multiple cruise missile system, it is essential that actuator failures should be considered in the design of the guidance loop, which provides the fault-tolerant acceleration output as the control objects of the control loop. Consequently actuator failures should be introduced into the kinematic model of the multiple cruise missile system.

Fig. 2 shows the formation tracking process for the cruise missile system.

The kinematic model of the multiple cruise missile system can be depicted by the second-order system. A second-order multiple cruise missile system with a leader and N followers is considered, where followers suffer from actuator failures.

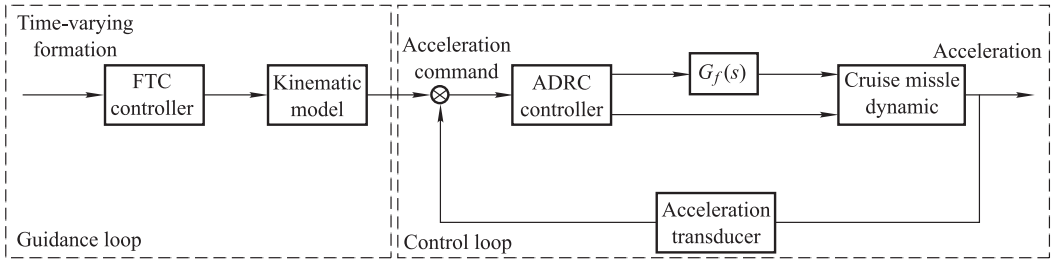

Fig. 2 Formation tracking process for the multiple cruise missile system

The control purpose is to allow the total of N followers to realize the specified time-varying FTC formation shape and follow up the motion trajectory generated by the only leader in the event of actuator failures.

The kinematic model of the N followers are given as

$$\begin{cases} \dot{\boldsymbol{x}}_i(t) = \boldsymbol{v}_i(t) \\ \dot{\boldsymbol{v}}_i(t) = \boldsymbol{g}_i(t)\boldsymbol{u}_i(t) + \boldsymbol{b}_i(t) \end{cases} \tag{5}$$

where $n \geqslant 1$ is the dimension of the space, $\boldsymbol{x}_i(t) \in \mathbf{R}^n$ is the position, $\boldsymbol{v}_i(t) \in \mathbf{R}^n$ denotes the velocity, and $\boldsymbol{u}_i(t) \in \mathbf{R}^n$ stands for the control input vector of the agent i respectively. $\boldsymbol{g}_i(t) = \mathrm{diag}\{g_{i1}(t), g_{i2}(t), \ldots, g_{in}(t)\}$ and $\boldsymbol{b}_i(t) = [b_{i1}(t), b_{i2}(t), \ldots, b_{in}(t)]^{\mathrm{T}}$, where $0 < g_{ij}(t) \leqslant 1$ denotes the unknown gain failure and $b_{ij}(t)$ represents the unknown bias failure of the actuator channel j ($j = 1, \ldots, n$) with regard to the follower i ($i = 1, \ldots, N$).

For the sake of simplicity in description, if not otherwise specified, n is assumed to be 1. Whereas, all the following results can be extended directly to a higher dimensional situation by way of the Kronecker product.

Table 2 presents the actuator failure modes of different agents for the multiple cruise missile system in this paper.

Table 2 Actuator failure modes of different agents

Actuator failure modes	Bias failure parameter	Gain failure parameter
Gain failure	$\|\boldsymbol{b}_i(t)\| = 0$	$0 < \|\boldsymbol{g}_i(t)\| < 1$
Bias failure	$\|\boldsymbol{b}_i(t)\| \neq 0$	$\|\boldsymbol{g}_i(t)\| = 1$
Both failure and bias failure	$\|\boldsymbol{b}_i(t)\| \neq 0$	$0 < \|\boldsymbol{g}_i(t)\| < 1$
Fault-free	$\|\boldsymbol{b}_i(t)\| = 0$	$\|\boldsymbol{g}_i(t)\| = 1$

Assumption 2 Time-varying bias failure and gain failure parameters $\boldsymbol{b}_i(t)$ and $\boldsymbol{g}_i(t)$ are given to be unknown and bounded, while there are unknown positive constants $\overline{b}_i$ and $\underline{g}_i$ such that $\|\boldsymbol{b}_i(t)\| \leqslant \overline{b}_i, 0 < \underline{g}_i \leqslant \|\boldsymbol{g}_i(t)\| \leqslant 1$ ($i = 1, \ldots, N$).

Assumption 3 The directed communication interaction topology $\boldsymbol{G}$ for the multiple cruise missile system is connected.

The time-varying FTC formation for the followers is determined by a vector $\boldsymbol{f}_F(t) = [\boldsymbol{f}_1^{\mathrm{T}}(t), \boldsymbol{f}_2^{\mathrm{T}}(t), \ldots, \boldsymbol{f}_N^{\mathrm{T}}(t)]^{\mathrm{T}}$, in which $\boldsymbol{f}_i(t) = [\boldsymbol{f}_{ix}(t), \boldsymbol{f}_{iv}(t)]^{\mathrm{T}}$ ($i \in F$) can

be piecewise continuously differentiable for the follower i with $\boldsymbol{f}_{ix}(t)$ and $\boldsymbol{f}_{iv}(t)$ being the components of $\boldsymbol{h}_i(t)$ in regard to the states of position and velocity, respectively.

Let $\boldsymbol{s}_k(t) = [x_k(t), v_k(t)]^{\mathrm{T}}$ $(k = 1, \ldots, N+1)$.

Definition 1 The multi-agent system (5) is called to realize time-varying FTC formation for any specified bounded initial state, if

$$\lim_{t\to\infty}((\boldsymbol{s}_i(t)-\boldsymbol{f}_i(t))-(\boldsymbol{s}_j(t)-\boldsymbol{f}_j(t))) = \boldsymbol{0}_{2\times 1}, \quad i,j \in F. \tag{6}$$

Definition 2 The multi-agent system (5) is called to accomplish target enclosing for any specified bounded initial state, if

$$\lim_{t\to\infty}\left(\sum_{i=1}^{N}\boldsymbol{s}_i(t)/N - \boldsymbol{s}_{N+1}(t)\right) = \boldsymbol{0}_{2\times 1}, \quad i \in F. \tag{7}$$

Definition 3 The multi-agent system is called to accomplish time-varying FTC formation tracking if (6) and (7) hold simultaneously for any specified bounded initial state.

Let $\boldsymbol{f}_{N+1}(t) = \sum_{i=1}^{N}\boldsymbol{f}_i(t)/N$, thus $\boldsymbol{f}_{N+1}(t) = 0$ by choosing $\lim_{t\to\infty}\sum_{i=1}^{N}\boldsymbol{f}_i(t) = \boldsymbol{0}_{2\times 1}$. Then the time-varying vector $\boldsymbol{f}(t) = [\boldsymbol{f}_1^{\mathrm{T}}(t), \ldots, \boldsymbol{f}_{N+1}^{\mathrm{T}}(t)]$ determines the time-varying FTC formation tracking shape for the multiple cruise missile system.

3. Main results

This section deals with the FTC formation tracking guidance loop and control loop design for the multiple cruise missile system respectively. Fault-tolerant protocols to realize the time-varying FTC formation tracking are firstly put forward in the guidance loop. Thus sufficient conditions and an approach to fix the parameters in the protocols are investigated. An ESO is used to calculate the unknown dynamic characteristics of the turbojet engine and compensate for it online in the control loop. A distributed control scheme by way of the ADRC is further studied for each cruise missile, which guarantees acceleration track of the guidance output signals in finite time.

3.1 Formation tracking guidance loop design

For the multiple cruise missile system (5), time-varying FTC formation tracking protocols are designed as follows:

$$\begin{cases} \boldsymbol{u}_i(t) = -\widehat{\boldsymbol{\sigma}}_i(t)(1+\|\dot{\boldsymbol{f}}_{iv}(t)\|)\mathrm{sgn}(\boldsymbol{\delta}_i(t)) - \widehat{\boldsymbol{\sigma}}_i(t)\boldsymbol{\delta}_i(t) \\ \dot{\widehat{\boldsymbol{\sigma}}}_i(t) = \boldsymbol{\tau}_i(1+\|\dot{\boldsymbol{f}}_{iv}(t)\|)\|\boldsymbol{\delta}_i(t)\| + \boldsymbol{\tau}_i\|\boldsymbol{\delta}_i(t)\|^2 \end{cases} \tag{8}$$

where $i \in 1, \ldots, N$.

Let

$$\boldsymbol{\delta}_i(t) = \boldsymbol{v}_i(t) - \boldsymbol{f}_{iv}(t) + \sum_{j=1}^{N+1} w_{ij}((\boldsymbol{x}_i(t) - \boldsymbol{f}_{ix}(t)) - (\boldsymbol{x}_j(t) - \boldsymbol{f}_{jx}(t))),$$

$\widehat{\sigma}_i(t)$ denotes an adaptive parameter that varies with time, the sign function of $\boldsymbol{\delta}_i(t)$ can be expressed as $\mathrm{sgn}(\boldsymbol{\delta}_i(t))$, and τ_i represents a non-negative value to be devised later, $i = 1, \ldots, N$.

Remark 1 Protocols (8) are a node-based formation tracking method, which can be specified free from the global information about the directed graph and actuator malfunctions. The time-varying FTC formation tracking protocol for this second-order multiple cruise missile system is proposed in [15], but protocol (3) in [15] is not available in this paper because actuator malfunctions are not taken into account therein, and the time-varying formation's derivative achieves in vain to be offset directly through the control input. Fault-tolerant formation tracking protocols (8) are provided for the multiple cruise missile system (5) utilizing the adaptive updating mechanism to adapt to the actuator bias failure and gain failure, as well as complementing the time-varying FTC formation' derivative and avoiding the calculation of these non-zero eigenvalue for the Laplacian matrix. It should be noted that real-time location information of the targeted moving object plays an irreplaceable role in the determination of the protocol $\boldsymbol{u}_i(t)$ $(i = 1, \ldots, N)$. Moreover, estimation of the target motion state can be achieved through a Gaussian-sum based cubature Kalman filter (see e.g., [40,41] and the academic studies therein).

In this paper, the following two problems for the multiple cruise missile system (5) under directed topologies and protocols (8) in the event of actuator malfunctions are mainly dealt with: (i) in what cases the time-varying FTC formation tracking will be accomplished; (ii) how to construct fault-tolerant protocols (8) to realize the time-varying control and guidance FTC formation tracking.

Theorem 1 The multiple cruise missile system (5) under protocols (8) accomplishes time-varying FTC tracking if this following case holds.

For any $i \in F$, $\lim_{t\to\infty}(\boldsymbol{f}_{iv}(t) - \dot{\boldsymbol{f}}_{ix}(t)) = 0$.

Proof Let $\boldsymbol{\chi}_i(t) = \boldsymbol{x}_i(t) - \boldsymbol{f}_{ix}(t)$ and $\boldsymbol{\tau}_i(t) = \boldsymbol{v}_i(t) - \boldsymbol{f}_{iv}(t)$ $(i = 1, \ldots, N+1)$. Then the multiple cruise missile system (5) can be translated in this following format:

$$\begin{cases} \dot{\boldsymbol{\chi}}_i(t) = \boldsymbol{\tau}_i(t) + \boldsymbol{f}_{iv}(t) - \dot{\boldsymbol{f}}_{ix}(t) \\ \dot{\boldsymbol{\tau}}_i(t) = g_i(t)\boldsymbol{u}_i(t) + \boldsymbol{b}_i(t) - \dot{\boldsymbol{f}}_{iv}(t) \end{cases} \tag{9}$$

Let

$$\overline{\boldsymbol{\chi}}_i(t) = -\sum_{j=1}^{N+1} \varepsilon_j \boldsymbol{\chi}_j(t) + \boldsymbol{\chi}_i(t)$$

$$\widetilde{\boldsymbol{\chi}}_i(t) = [\widetilde{\boldsymbol{\chi}}_1^{\mathrm{T}}(t), \dots, \widetilde{\boldsymbol{\chi}}_{N+1}^{\mathrm{T}}(t)]^{\mathrm{T}}$$

$$\boldsymbol{\delta}(t) = [\boldsymbol{\delta}_1^{\mathrm{T}}(t), \dots, \boldsymbol{\delta}_{N+1}^{\mathrm{T}}(t)]^{\mathrm{T}}$$

$$\boldsymbol{g}(t) = [\boldsymbol{g}_1^{\mathrm{T}}(t), \dots, \boldsymbol{g}_{N+1}^{\mathrm{T}}(t)]^{\mathrm{T}}$$

$$\boldsymbol{b}(t) = [\boldsymbol{b}_1^{\mathrm{T}}(t), \dots, \boldsymbol{b}_{N+1}^{\mathrm{T}}(t)]^{\mathrm{T}}$$

$$\dot{\boldsymbol{f}}_v(t) = [\dot{\boldsymbol{f}}_{1v}^{\mathrm{T}}(t), \dots, \dot{\boldsymbol{f}}_{N+1v}^{\mathrm{T}}(t)]^{\mathrm{T}}$$

where ε_j is denoted in Lemma 1.

Thus the multiple cruise missile system (9) can be translated into

$$\begin{cases} \dot{\widetilde{\boldsymbol{\chi}}}(t) = (\boldsymbol{I}_N - \boldsymbol{1}_N \boldsymbol{\varepsilon}^{\mathrm{T}})\boldsymbol{\delta}(t) - \boldsymbol{L}\widetilde{\boldsymbol{\chi}}(t) \\ \dot{\boldsymbol{\delta}}(t) = -\boldsymbol{g}(t)\boldsymbol{\delta}(t)\boldsymbol{\sigma}(t) + \boldsymbol{L}\boldsymbol{\delta}(t) - \boldsymbol{L}^2\widetilde{\boldsymbol{\chi}}(t) \\ -\boldsymbol{g}(t)\widehat{\boldsymbol{\eta}}(t)\mathrm{sgn}(\boldsymbol{\delta}(t)) - \dot{\boldsymbol{f}}_v(t) + \boldsymbol{b}(t) \end{cases} \tag{10}$$

where

$$\widehat{\eta}_i(t) = (1 + \|\dot{\boldsymbol{f}}_{iv}(t)\|)\widehat{\boldsymbol{\sigma}}_i(t),$$

$$\widehat{\boldsymbol{\sigma}}(t) = \mathrm{diag}\{\widehat{\sigma}_1(t), \dots, \widehat{\sigma}_{N+1}(t)\},$$

$$\widehat{\boldsymbol{\eta}}(t) = \mathrm{diag}\{\widehat{\eta}_1(t), \dots, \widehat{\eta}_{N+1}(t)\}, \quad i = 1, \dots, N+1.$$

The Lyapunov candidate function is chosen as

$$V(t) = \widetilde{\boldsymbol{\chi}}^{\mathrm{T}}(t)\boldsymbol{\Gamma}\widetilde{\boldsymbol{\chi}}(t) + \frac{1}{2}\boldsymbol{\delta}^{\mathrm{T}}(t)\boldsymbol{\delta}(t) + \sum_{i=1}^{N+1} \frac{\underline{g}_i \widetilde{\boldsymbol{\sigma}}_i^2(t)}{2\tau_i} \tag{11}$$

where $\widehat{\sigma}_i(t) - \overline{\sigma}$ is denoted by $\widetilde{\boldsymbol{\sigma}}_i(t)$, $\overline{\sigma}$ is a non-negative constant to be fixed later, and $\boldsymbol{\Gamma} = \mathrm{diag}\{\varepsilon_1, \dots, \varepsilon_{N+1}\}$.

$V(t)$'s time derivative along (10)'s trajectory can be computed as follows:

$$\dot{V}(t) = \boldsymbol{\delta}^{\mathrm{T}}(t)\boldsymbol{L}\boldsymbol{\delta}(t) + 2\widetilde{\boldsymbol{\chi}}^{\mathrm{T}}(t)(\boldsymbol{\Gamma} - \boldsymbol{\varepsilon}\boldsymbol{\varepsilon}^{\mathrm{T}})\boldsymbol{\delta}(t) - \boldsymbol{\delta}^{\mathrm{T}}(t)\boldsymbol{L}^2\widetilde{\boldsymbol{\chi}}(t) - \boldsymbol{\delta}^{\mathrm{T}}(t)\widehat{\boldsymbol{\sigma}}(t)\boldsymbol{g}(t)\boldsymbol{\delta}(t) + \boldsymbol{b}(t)\boldsymbol{\delta}^{\mathrm{T}}(t) -$$

$$\widetilde{\boldsymbol{\chi}}^{\mathrm{T}}(t)\widehat{\boldsymbol{L}}\widetilde{\boldsymbol{\chi}}(t) - \boldsymbol{\delta}^{\mathrm{T}}(t)\dot{\boldsymbol{h}}_v(t) - \boldsymbol{\delta}^{\mathrm{T}}(t)\widehat{\boldsymbol{\eta}}(t)\boldsymbol{g}(t)\mathrm{sgn}(\boldsymbol{\delta}(t)) + \sum_{i=1}^{N+1} \underline{g}_i(t)\widetilde{\boldsymbol{\sigma}}_i(t)((1 + \|\dot{\boldsymbol{f}}_{iv}(t)\|)\|\boldsymbol{\delta}_i(t)\| + \boldsymbol{\delta}_i^{\mathrm{T}}(t)\boldsymbol{\delta}_i(t)) \tag{12}$$

where $\widehat{\boldsymbol{L}} = \boldsymbol{\Gamma}\boldsymbol{L} + \boldsymbol{L}^{\mathrm{T}}\boldsymbol{\Gamma}$.

Based upon Assumption 2, it can be concluded that

$$-\boldsymbol{\delta}^{\mathrm{T}}(t)\widehat{\boldsymbol{\sigma}}(t)\boldsymbol{g}(t)\boldsymbol{\delta}(t) = -\sum_{i=1}^{N+1} \boldsymbol{\delta}_i^{\mathrm{T}}(t)\widehat{\boldsymbol{\sigma}}_i(t)\boldsymbol{g}_i(t)\boldsymbol{\delta}_i(t) \leqslant -\sum_{i=1}^{N+1} \underline{g}_i \widehat{\boldsymbol{\sigma}}_i(t)\boldsymbol{\delta}_i^{\mathrm{T}}(t)\boldsymbol{\delta}_i(t) \tag{13}$$

$$\boldsymbol{b}(t)\boldsymbol{\delta}^{\mathrm{T}}(t) \leqslant \sum_{i=1}^{N+1} \|\boldsymbol{b}_i(t)\|\|\boldsymbol{\delta}_i(t)\| \leqslant \sum_{i=1}^{N+1} \overline{b}_i\|\boldsymbol{\delta}_i(t)\|. \tag{14}$$

From (12)–(14), one can get

$$\dot{V}(t) \leqslant \boldsymbol{\delta}^{\mathrm{T}}(t)\boldsymbol{L}\boldsymbol{\delta}(t) + 2\widetilde{\boldsymbol{\chi}}^{\mathrm{T}}(t)(\boldsymbol{\Gamma} - \boldsymbol{\varepsilon}\boldsymbol{\varepsilon}^{\mathrm{T}})\boldsymbol{\delta}(t) - \widetilde{\boldsymbol{\chi}}^{\mathrm{T}}(t)\widehat{\boldsymbol{L}}\widetilde{\boldsymbol{\chi}}(t) - \boldsymbol{\delta}^{\mathrm{T}}(t)\dot{\boldsymbol{f}}_v(t) -$$

$$\boldsymbol{\delta}^{\mathrm{T}}(t)\boldsymbol{g}(t)\widehat{\boldsymbol{\eta}}(t)\mathrm{sgn}(\boldsymbol{\delta}(t)) - \boldsymbol{\delta}^{\mathrm{T}}(t)\boldsymbol{L}^2\widetilde{\boldsymbol{\chi}}(t) - \sum_{i=1}^{N+1} \underline{g}_i \widehat{\boldsymbol{\sigma}}_i(t)\boldsymbol{\delta}_i^{\mathrm{T}}(t)\boldsymbol{\delta}_i(t) + \sum_{i=1}^{N+1} \overline{b}_i\|\boldsymbol{\delta}_i(t)\| +$$

$$\sum_{i=1}^{N} \underline{g}_i(t)\widetilde{\boldsymbol{\sigma}}_i(t)((1 + \|\dot{\boldsymbol{f}}_{iv}(t)\|)\|\boldsymbol{\delta}_i(t)\| + \boldsymbol{\delta}_i^{\mathrm{T}}(t)\boldsymbol{\delta}_i(t)) \leqslant \boldsymbol{\delta}^{\mathrm{T}}(t)\boldsymbol{L}\boldsymbol{\delta}(t) + 2\widetilde{\boldsymbol{\chi}}^{\mathrm{T}}(t)(\boldsymbol{\Gamma} - \boldsymbol{\varepsilon}\boldsymbol{\varepsilon}^{\mathrm{T}})\boldsymbol{\delta}(t) -$$

$$\widetilde{\boldsymbol{\chi}}^{\mathrm{T}}(t)\widehat{\boldsymbol{L}}\widetilde{\boldsymbol{\chi}}(t) + \sum_{i=1}^{N+1} \|\dot{\boldsymbol{f}}_{iv}(t)\|\|\boldsymbol{\delta}_i(t)\| - \boldsymbol{\delta}^{\mathrm{T}}(t)\boldsymbol{g}(t)\widehat{\boldsymbol{\eta}}(t)\mathrm{sgn}(\boldsymbol{\delta}(t)) - \boldsymbol{\delta}^{\mathrm{T}}(t)\boldsymbol{L}^2\widetilde{\boldsymbol{\chi}}(t) - \sum_{i=1}^{N+1} \underline{g}_i \widehat{\boldsymbol{\sigma}}_i(t)\boldsymbol{\delta}_i^{\mathrm{T}}(t)\boldsymbol{\delta}_i(t) + \sum_{i=1}^{N} \overline{b}_i\|\boldsymbol{\delta}_i(t)\| +$$

$$\sum_{i=1}^{N+1} \underline{g}_i(t)\widetilde{\boldsymbol{\sigma}}_i(t)((1 + \|\dot{\boldsymbol{f}}_{iv}(t)\|)\|\boldsymbol{\delta}_i(t)\| + \boldsymbol{\delta}_i^{\mathrm{T}}(t)\boldsymbol{\delta}_i(t)). \tag{15}$$

since

$$-\boldsymbol{\delta}^{\mathrm{T}}(t)\boldsymbol{g}(t)\widehat{\boldsymbol{\eta}}(t)\mathrm{sgn}(\boldsymbol{\delta}(t)) = -\sum_{i=1}^{N+1} (1 + \|\dot{\boldsymbol{f}}_{iv}(t)\|)\boldsymbol{\delta}_i^{\mathrm{T}}(t)\boldsymbol{g}_i(t)\widehat{\boldsymbol{\sigma}}_i(t)\mathrm{sgn}(\boldsymbol{\delta}_i(t)) \leqslant$$

$$-\sum_{i=1}^{N+1} (1 + \|\dot{\boldsymbol{f}}_{iv}(t)\|)\underline{g}_i \widehat{\sigma}_i(t)\|\boldsymbol{\delta}_i(t)\| \tag{16}$$

$$2\widetilde{\boldsymbol{\chi}}^{\mathrm{T}}(\boldsymbol{\Gamma}-\boldsymbol{\varepsilon}\boldsymbol{\varepsilon}^{\mathrm{T}})\boldsymbol{\delta}\leqslant 2\|\boldsymbol{\delta}\|\|\widetilde{\boldsymbol{\chi}}\| \tag{17}$$

$$\boldsymbol{\delta}^{\mathrm{T}}\boldsymbol{L}\boldsymbol{\delta}\leqslant\|\boldsymbol{\delta}\|\|\boldsymbol{L}\boldsymbol{\delta}\|\leqslant\sigma_{\max}(\boldsymbol{L})\|\boldsymbol{\delta}\|^2 \tag{18}$$

$$-\boldsymbol{\delta}^{\mathrm{T}}\boldsymbol{L}^2\widetilde{\boldsymbol{\chi}}\leqslant\sigma_{\max}^2(\boldsymbol{L})\|\boldsymbol{\delta}\|\|\widetilde{\boldsymbol{\chi}}\|. \tag{19}$$

Putting together (16) – (19) and based upon (15) results in

$$\dot{V}(t)\leqslant(\sigma_{\max}(\boldsymbol{L})-\underline{g}\overline{\sigma})\|\boldsymbol{\delta}(t)\|^2+2\|\boldsymbol{\delta}(t)\|\|\widetilde{\boldsymbol{\chi}}(t)\|-\widetilde{\boldsymbol{\chi}}^{\mathrm{T}}(t)\widehat{\boldsymbol{L}}\widetilde{\boldsymbol{\chi}}(t)+\sigma_{\max}^2(\boldsymbol{L})\|\boldsymbol{\delta}(t)\|\|\widetilde{\boldsymbol{\chi}}(t)\|-$$
$$\sum_{i=1}^{N+1}(\underline{g}_i\overline{\sigma}-1)\|\dot{\boldsymbol{f}}_{iv}(t)\|\|\boldsymbol{\delta}_i\|-\sum_{i=1}^{N+1}(\underline{g}_i\overline{c}-\overline{b}_i)\|\boldsymbol{\delta}_i\|. \tag{20}$$

Note that $\widetilde{\boldsymbol{\chi}}^{\mathrm{T}}\boldsymbol{\varepsilon}=0$ and $\boldsymbol{\varepsilon}>\boldsymbol{0}$, based on Lemma 1 and Assumption 3, one obtains

$$\widetilde{\boldsymbol{\chi}}^{\mathrm{T}}(t)\widehat{\boldsymbol{L}}\widetilde{\boldsymbol{\chi}}(t)>\frac{\lambda_2(\widehat{\boldsymbol{L}})}{N+1}\|\widetilde{\boldsymbol{\chi}}\|^2. \tag{21}$$

Moreover,

$$\sigma_{\max}^2(\boldsymbol{L})\|\widetilde{\boldsymbol{\chi}}\|\|\boldsymbol{\delta}\|\leqslant\lambda_2(\widehat{\boldsymbol{L}})\frac{\|\widetilde{\boldsymbol{\chi}}\|^2}{4(N+1)}+\sigma_{\max}^4(\boldsymbol{L})\frac{N\|\boldsymbol{\delta}\|^2}{\lambda_2(\widehat{\boldsymbol{L}})} \tag{22}$$

$$2\|\boldsymbol{\delta}(t)\|\|\widetilde{\boldsymbol{\chi}}(t)\|\leqslant\frac{\lambda_2(\widehat{\boldsymbol{L}})}{4(N+1)}\|\widetilde{\boldsymbol{\chi}}(t)\|^2+\frac{4(N+1)}{\lambda_2(\widehat{\boldsymbol{L}})}\|\boldsymbol{\delta}(t)\|^2. \tag{23}$$

Substitute (21) – (23) into (20), one can get

$$\dot{V}\leqslant-\frac{\lambda_2(\widehat{\boldsymbol{L}})}{2(N+1)}\|\widetilde{\boldsymbol{\chi}}(t)\|^2-\left(-\sigma_{\max}(\boldsymbol{L})-\frac{(N+1)(\sigma_{\max}^4(\boldsymbol{L})+4)}{\lambda_2(\widehat{\boldsymbol{L}})}+\underline{g}\overline{\sigma}\right)\|\boldsymbol{\delta}(t)\|^2-$$
$$\sum_{i=1}^{N+1}\|\dot{\boldsymbol{f}}_{iv}(t)\|(\underline{g}_i\overline{\sigma}-1)\|\boldsymbol{\delta}_i(t)\|-\sum_{i=1}^{N+1}(\underline{g}_i\overline{\sigma}-\overline{b}_i)\|\boldsymbol{\delta}_i(t)\|. \tag{24}$$

Let

$$\overline{\sigma}>\max\left\{\frac{1}{\underline{g}}\left(\frac{(N+1)(\sigma_{\max}^4(\boldsymbol{L})+4)}{\lambda_2(\widehat{\boldsymbol{L}})}+\sigma_{\max}(\boldsymbol{L})\right),\frac{1}{\underline{g}},\frac{\overline{b}_i}{\underline{g}_i}\right\},\quad i=1,\ldots,N+1. \tag{25}$$

Accordingly, we can infer that $\dot{V}(t)\leqslant 0$. Besides, it can be implied that $\widetilde{\boldsymbol{\chi}}(t)=0$, $\boldsymbol{\delta}(t)=0$ since $\dot{V}(t)\equiv 0$. One can also see that $\lim\limits_{t\to\infty}(\boldsymbol{\chi}_i(t)-\boldsymbol{\chi}_j(t))=0$, $\lim\limits_{t\to\infty}(\boldsymbol{\tau}_i(t)-\boldsymbol{\tau}_j(t))=0$ $(i,j=1,\ldots,N+1)$. Hence, the adaptive gain $\widehat{\boldsymbol{\sigma}}_i(t)$ and these time-varying FTC formation tracking errors $\boldsymbol{\delta}(t)$ and $\widetilde{\boldsymbol{\chi}}(t)$ are assumed to be uniformly ultimately bounded. Therefore, the multiple cruise missile system (5) under protocols (8) in the presence of actuator malfunctions can accomplish time-varying FTC formation tracking in the end. Furthermore, (25) gives an effective method for determining the positive constant $\overline{\sigma}$ of protocols (8). Theorem 1 is completed. □

3.2 Formation tracking control loop design

The cruise missile horizontal dynamics (1) can be rewritten as

$$\begin{cases}\dot{v}_x=(P_0\cos\alpha-C_xqS)/m+P_1\phi\cos\alpha/m+d\cos\alpha\\ \dot{v}_z=g\tan\gamma_v\\ (P\sin\alpha+C_yqS)\cos\gamma_v=mg\\ \ddot{\phi}=\omega_n^2\phi_C-2\xi\omega_n\dot{\phi}-\omega_n^2\phi\end{cases}. \tag{26}$$

As mentioned earlier, the input of (26) is chosen as ϕ and γ_v. Intuitively, ϕ can be designed primarily to control the thrust, hence the acceleration in the X direction, whereas γ_v will be utilized to modulate the acceleration in the Z direction.

During the controller development for the cruise missile bank angle γ_v, it is necessary to take the dynamic lag modeled by a low-pass filter into account. Then the PI controller devised for the bank angle motion is designed as

$$\gamma_v=(\tan^{-1}(\dot{v}_{zc}/g)-k_{Pz}(\dot{v}_z-\dot{v}_{zc})-$$
$$k_{Iz}\int(\dot{v}_z-\dot{v}_{zc})\mathrm{d}t-k_{Dz}(\ddot{v}_z-\ddot{v}_{zc}))\frac{1}{0.8s+1} \tag{27}$$

where $\dot{v}_{zc}$ is the acceleration to be controlled in the Z direction designed by (8).

For the purposes of the engine throttle ϕ_C control design, let $x_2=h(x_1)=\dfrac{P_0\cos\alpha-C_xqS}{m}+d\cos\alpha$ be an extended state of the system and assume $\dot{x}_2=\omega(t)=\dfrac{\mathrm{d}((P_0\cos\alpha-C_xqS)/m+d\cos\alpha)}{\mathrm{d}t}$. Then the dynamics

for the acceleration along the X direction tracking appearing in (26) can be expressed as

$$\begin{cases} \dot{x}_1 = h(x_1) + bu \\ \dot{x}_2 = \omega(t) \\ y = x_1 \end{cases} \tag{28}$$

where $x_1 = v_x$, $b = \dfrac{P_1 \cos\alpha}{m}$ and $u = \phi$ is the state of the system, the known structural parameter and the control input respectively. An ESO is correspondingly proposed for (28):

$$\begin{cases} e = z_1 - y \\ \dot{z}_1 = z_2 - \beta_{01} e + bu \\ z_2 = -\beta_{02} |e|^{\frac{1}{2}} \mathrm{sign}(e) \end{cases} \tag{29}$$

where $[z_1, z_2]^{\mathrm{T}}$ is the ESO state, and β_{01} and β_{02} are some constants to be chosen. The above is a general form of the ESO proposed in [42].

Associated with the system (28) and the ESO (29), we denote $[e_1, e_2]^{\mathrm{T}}$ with

$$e_i = z_i - x_i, \quad i = 1, 2. \tag{30}$$

Then the error state equation can be expressed as

$$\begin{cases} \dot{e}_1 = e_2 - \beta_{01} e_1 \\ \dot{e}_2 = \omega - \beta_{02} |e_1|^{\frac{1}{2}} \mathrm{sign}(e_1) \end{cases}. \tag{31}$$

We anticipate that the right hand sides of (31) equal zero as

$$|e_1| = \left(\frac{\omega}{\beta_{02}}\right)^2, \quad |e_2| = \beta_{01} \left(\frac{\omega}{\beta_{02}}\right)^2. \tag{32}$$

Note that elements of the errors can be specified as $\beta_{02} \gg \omega$, then e_1 and e_2 converge to 0 ultimately, that is $z_i \to x_i$ $(i = 1, 2)$ as $\beta_{02} \gg \omega$, $t \to \infty$. Then one can obtain the ADRC law, as shown in Fig. 3.

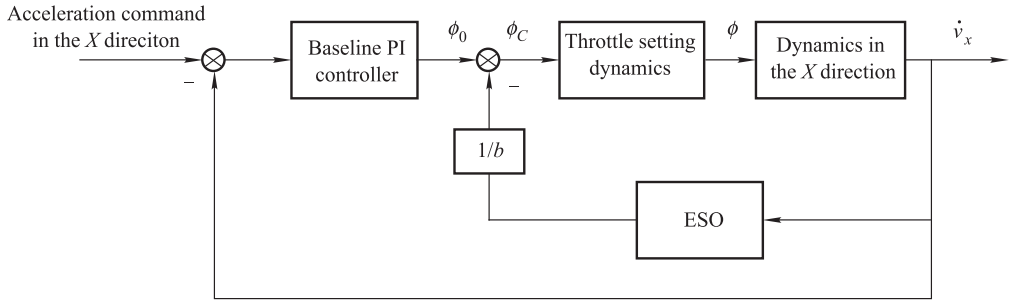

Fig. 3 Configuration of ADRC controller

In this case, utilizing the output of the ESO, the ADRC law is given by

$$u = u_0 - \frac{z_2(t)}{b} \tag{33}$$

where u_0 is the baseline PI controller to be designed:

$$u_0 = -k_{px}(\dot{v}_x - \dot{v}_{xc}) - k_{ix} \int (\dot{v}_x - \dot{v}_{xc}) \mathrm{d}t. \tag{34}$$

Substitution of (34) into (33) yields

$$\phi_C = u = \frac{-z_2}{P_1 \cos\alpha / m} - k_{px}(\dot{v}_x - \dot{v}_{xc}) - k_{ix} \int (\dot{v}_x - \dot{v}_{xc}) \mathrm{d}t \tag{35}$$

where $\dot{v}_{xc}$ is acceleration to be controlled in the X direction designed by (8).

Remark 2 The closed-loop system (28) is reduced to a linear one that incorporates with the estimation of the extended state due to the ADRC law (33). Acceleration tracking controller design for the second-order multiple cruise missile system is investigated in [15], but the PID controller in [15] is not applicable in that the coupling nonlinear dynamics are parts of the turbojet engine thrust modeling, and the effects of nonlinearities cannot be tolerated by the PID controller directly.

4. Simulation

To verify the proposed theories got in the previous sections, a numerical example is presented in this section. Each agent in this numerical simulation is assumed to stand for one cruise missile, the interaction communication topology for the multiple cruise missile system is illustrated in Fig. 4, which depicts a scenario where a cluster of Tomahawk cruise missiles attack Somali sea rover. Fig. 5 illustrates the motion estimation of the sea rover with a course angle $\gamma_T = 45^\circ$ and velocity $v_T = 50$ km/h through the Gaussian sum incremental Kalman filter. Assume that the interaction communication topology $\boldsymbol{G}$ has $0 - 1$ weights without loss of generality.

A second-order multiple cruise missile system with a leader and six followers is considered. The kinematic model of the six followers are determined by (5) with the position vector defined as $\boldsymbol{x}_i(t) = [x_{Xi}(t), x_{Zi}(t)]^{\mathrm{T}}$, the velocity vector denoted by $\boldsymbol{v}_i(t) = [v_{Xi}(t), v_{Zi}(t)]^{\mathrm{T}}$ and control input vector described as

$\boldsymbol{u}_i(t) = [u_{Xi}(t), u_{Zi}(t)]^{\mathrm{T}}$.

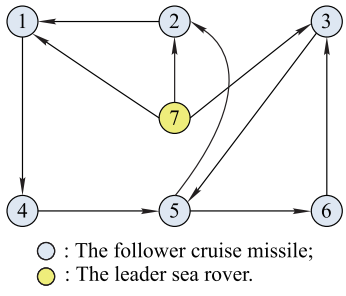

Fig. 4 Directed communication topology G

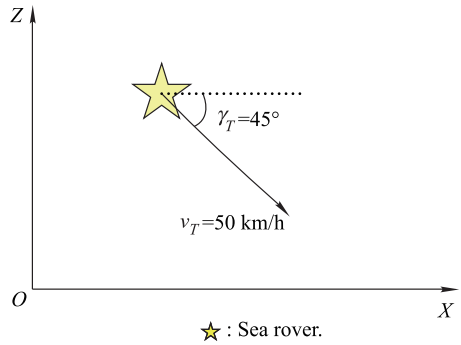

Fig. 5 Motion estimation of the sea rover

In order to demonstrate the validity of the theoretical strategy put forward in the paper, actuator failure modes are shown as follows. There are gain failure in cruise missile 6 and bias failure in cruise missile 3, cruise missiles 1, 2 and 4 are assumed to encounter both gain failures and bias failures, whereas cruise missile 5 is sound and trouble-free, as presented in Table 3.

These six followers will be driven to maintain the time-varying parallel hexagon FTC formation specified by $f_i(t)$ and rotate about the only leader meanwhile.

$$f_i(t) = \begin{bmatrix} 630\sin(0.4t + (i-1)\pi/3) \\ 252\cos(0.4t + (i-1)\pi/3) \\ 1\,890\cos(0.4t + (i-1)\pi/3) \\ -756\sin(0.4t + (i-1)\pi/3) \end{bmatrix},$$

$$i = 1, \ldots, 6; f_7(t) = 0. \tag{36}$$

If $f_i(t)$ $(i = 1, \ldots, 7)$ is accomplished, the states of the six followers will be located on the six vertices of the parallel hexagon along with rotating about the only leader with 0.4 rad/s as the angular velocity. Choose $\widehat{c}_{iX}(0) = 0$, $\widehat{c}_{iZ}(0) = 0$, $\gamma_{iX} = 1$, $\gamma_{iZ} = 1$.

Table 3 Cruise missiles actuator failure modes

Agent	Bias failure	Gain failure
Cruise missile1	$[0.2\cos(1.5t), -0.12\sin(3t)]^{\mathrm{T}}$	$\begin{bmatrix} 0.68 + 0.1\cos(t) & 0 \\ 0 & 0.8 - 0.11\sin(1.6t) \end{bmatrix}$
Cruise missile 2	$[-0.15\sin(2t), 0.1 - 0.1\cos(t)]^{\mathrm{T}}$	$\begin{bmatrix} 0.72 + 0.2\sin(2.1t) & 0 \\ 0 & 0.6 + 0.1\sin(t) \end{bmatrix}$
Cruise missile 3	$[-0.15\mathrm{e}^{-2t}, 0.2\sin(t)]^{\mathrm{T}}$	$\begin{bmatrix} 1 & 0 \\ 0 & 1 \end{bmatrix}$
Cruise missile 4	$[0.25\sin(3t), -0.23\cos(1.3t)]^{\mathrm{T}}$	$\begin{bmatrix} 0.65 + 0.15\cos(3t) & 0 \\ 0 & 0.8 - 0.1\sin(2t) \end{bmatrix}$
Cruise missile 5	$[0, 0]^{\mathrm{T}}$	$\begin{bmatrix} 1 & 0 \\ 0 & 1 \end{bmatrix}$
Cruise missile 6	$[0, 0]^{\mathrm{T}}$	$\begin{bmatrix} 0.85 - 0.1\sin(2t) & 0 \\ 0 & 0.7 + 0.2\mathrm{e}^{-3t} \end{bmatrix}$

Let the initial states of each cruise missile be determined by $s_{kl}(0) = 15\Theta - 7.5$ $(k = 1, \ldots, 7; l = 1, \ldots, 4)$, in which Θ denotes some pseudorandom constant distributed in 0 – 1. Moreover, Fig. 6 displays the adaptive gains $\widehat{c}_i(t)$ $(i = 1, 2, \ldots, 6)$. The states trajectory of position and velocity snapshots for these seven agents at different time periods can be found in Fig. 7 and Fig. 8, in which the leader is marked by pentagram, while the six followers are indicated by the asterisk, diamond, point, circle, square, triangle, respectively. Fig. 9 exhibits the expected acceleration tracking curves of a set of cruise missiles in the case of actuator malfunctions. We can easily conclude from Figs. 6 – 9 that both the states of positions and velocities components for the cruise missiles realize the predefined geometry along with revolving about the sea rover despite actuator malfunctions, which prove the validity of the designed approaches to carry on time-varying FTC formation tracking in the guidance loop design.

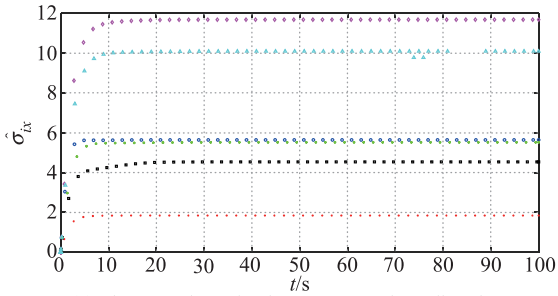

(a) Time-varying adaptive parameter in X direction

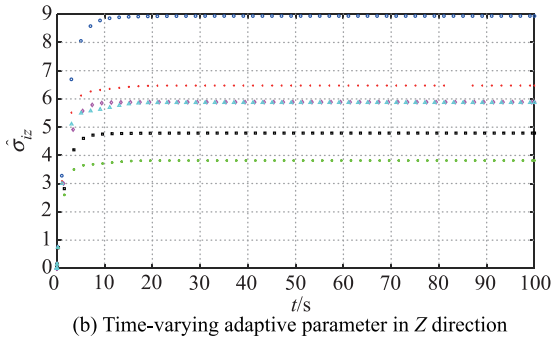

(b) Time-varying adaptive parameter in Z direction

∘ : Cruise missile 1; ◇ : Cruise missile 2; · : Cruise missile 3;
▫ : Cruise missile 4; · : Cruise missile 5; △ : Cruise missile 6.

Fig. 6 Variation curves of adaptive gains

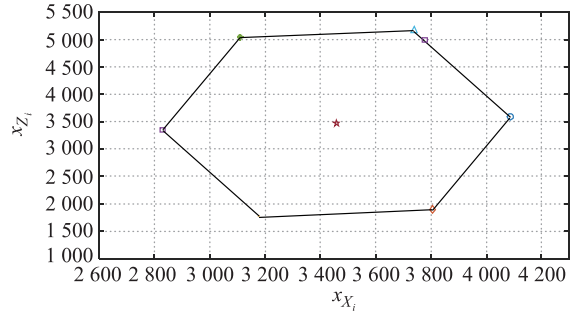

(c) t=98 s

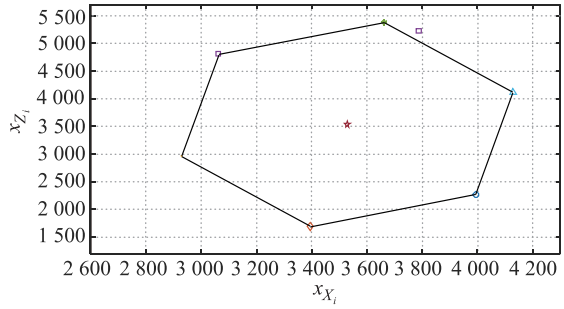

(d) t=100 s

∘ : Cruise missile 1; ◇ : Cruise missile 2; · : Cruise missile 3;
▫ : Cruise missile 4; · : Cruise missile 5; △ : Cruise missile 6;
★ : Sea rover.

Fig. 7 Snapshots of position trajectories at different time for these seven agents

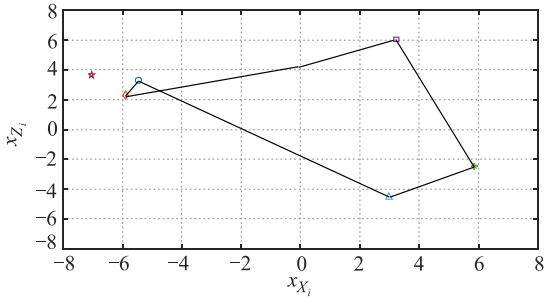

(a) t=0 s

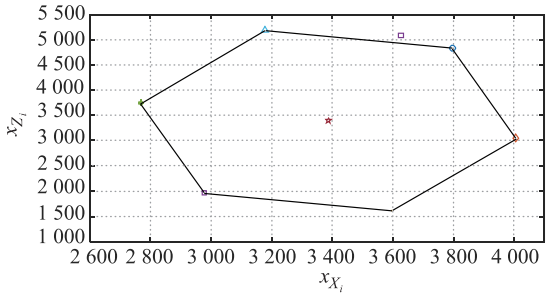

(b) t=96 s

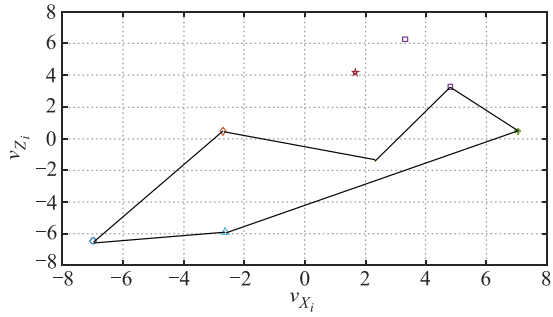

(a) t=0 s

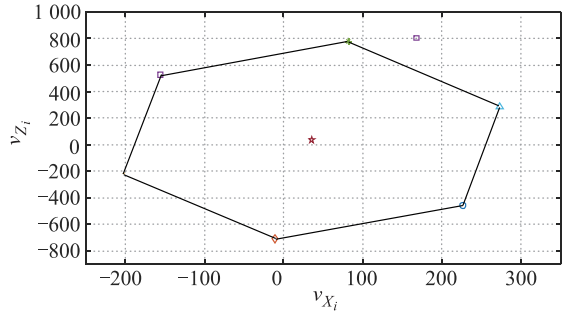

(b) t=96 s

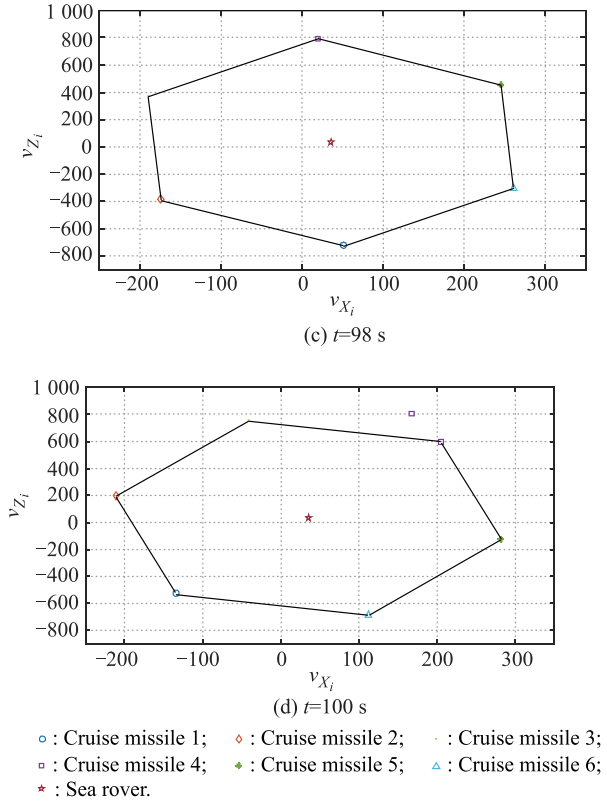

Fig. 8 Snapshots of velocity trajectories at different time for these seven agents

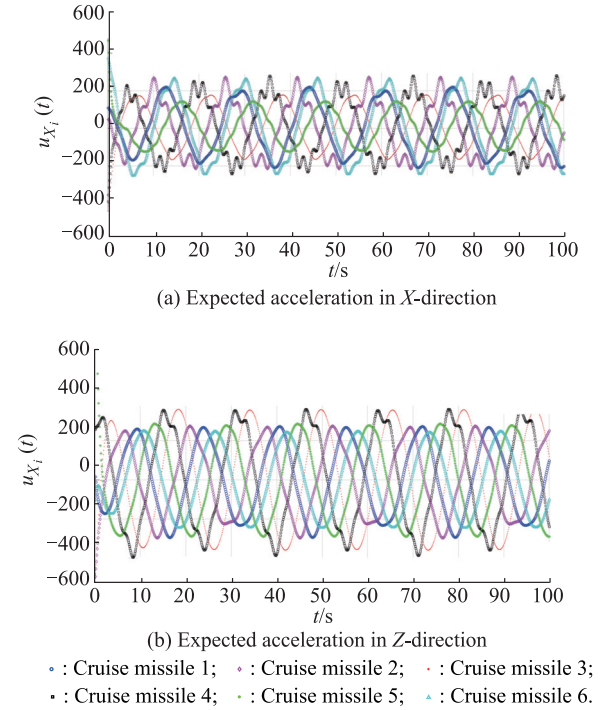

Fig. 9 Curves to track the expected acceleration

The application of the proposed ADRC and PI controller to the multiple cruise missile system is reflected in Figs. 10 – 13. The controller (27) and (35) are aimed at stabilizing the throttle setting of the turbojet engine and the motion form of the speed bank angle respectively, to follow up the reference inputs set up by the expected acceleration of each cruise missile. Taking cruise missile 1 as an example, the PI controller, with 0.3 and 0.5 as these effective coefficients designed to the proportional besides the integral terms separately, can meet the stabilization requirements for the speed bank angle. The ESO parameters of the ADRC controller for engine throttle setting is chosen as $\beta_{01} = 300$, $\beta_{02} = 1\,000$. Moreover, the proportional and integral terms belonging to the baseline PI controller are determined to be 12 and 10 respectively. Fig. 10 depicts that under the proposed control strategy, the output acceleration can trace the command acceleration effectively, whereas the proportion integration differentiation (PID) controller designed in [15] results in instability when applied to acceleration tracking in the X direction, as shown in Fig. 11. It can be obtained obviously by way of Fig. 12 and Fig. 13 that, this transition and amplitude for the controller output are quite stable and reasonable despite engine thrust modeling uncertainties, which manifest the practicability and potential of the developed methods for application in the aircraft design engineering.

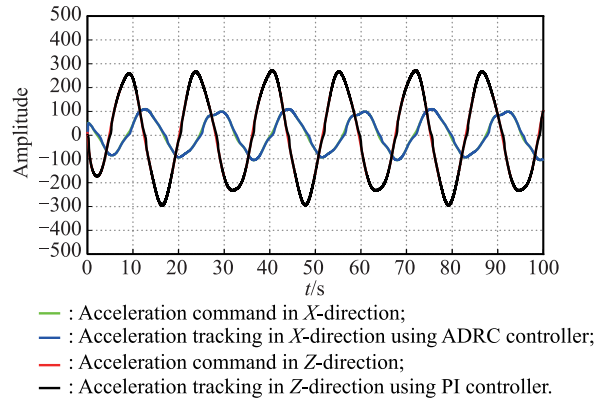

Fig. 10 Responses of acceleration for cruise missile 1 using controller (27) and (35)

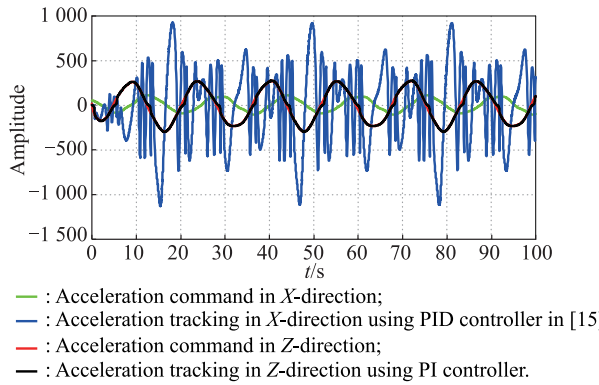

Fig. 11 Responses of acceleration for cruise missile 1 using PID controller in [15]

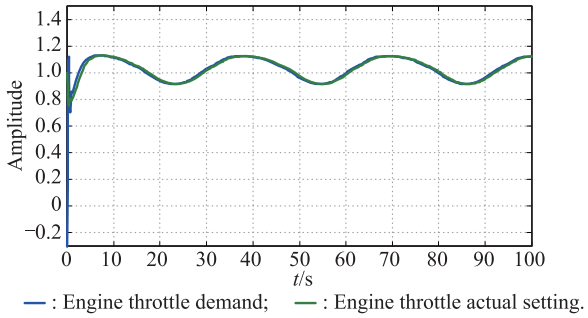

Fig. 12 Turbojet engine throttle setting

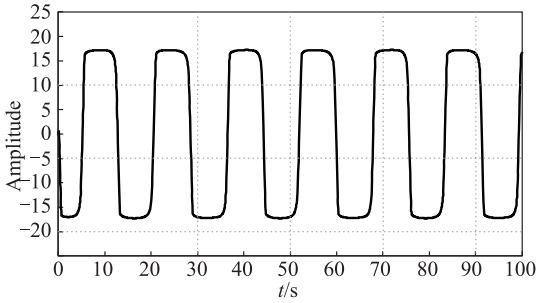

Fig. 13 Speed bank angle deflection

5. Conclusions

The time-varying fault-tolerant formation tracking problem for the multiple cruise missile system subjected to actuator failures and directed topologies is dealt with. The process to realize formation tracking for the multiple cruise missile system is divided into the guidance loop and the control loop. It is shown that with the proposed formation tracking protocols in the guidance loop design, the multi-agent system can not only compensate the uncharted actuator malfunctions, but also achieve the target enclosing ultimately. The obtained results are then applied to each cruise missile based on the ADRC by the way of acceleration tracking process. An interesting academic direction for the future is to extend fault-tolerant time-varying formation tracking protocols to the condition in which multi-agent systems are of heterogeneous dynamics and suffer from not only actuator failures but also sensor failures.

References

[1] DAS B, SUBUDHI B, PATI B B. Cooperative formation control of autonomous underwater vehicles: an overview. International Journal of Automation and Computing, 2016, 13(3): 199 – 225.

[2] PENG H, JIANG X. Nonlinear receding horizon guidance for spacecraft formation reconfiguration on libration point orbits using a symplectic numerical method. ISA Transactions, 2016, 60: 38 – 52.

[3] NIGAM N, BIENIAWSKI S, KROO I, et al. Control of multiple UAVs for persistent surveillance: algorithm and flight test results. IEEE Trans. on Control Systems Technology, 2012, 20(5): 1236 – 1251.

[4] DONG X W, YU B C, SHI Z Y, et al. Time-varying formation control for unmanned aerial vehicles: theories and applications. IEEE Trans. on Control Systems Technology, 2015, 23(1): 340 – 348.

[5] RAO S, GHOSE D. Sliding mode control-based autopilots for leaderless consensus of unmanned aerial vehicles. IEEE Trans. on Control Systems Technology, 2014, 2(5): 1964 – 1972.

[6] YOSHIDA K, FUKUSHIMA H, KON K, et al. Control of a group of mobile robots based on formation abstraction and decentralized locational optimization. IEEE Trans. on Robotics, 2017, 30(3): 550 – 565.

[7] QIN L, HE X, ZHOU D. Distributed proportion-integration-derivation formation control for second-order multi-agent systems with communication time delays. Neurocomputing, 2017, 267(6): 271 – 282.

[8] DU H B, CHENG Y Y, HE Y G. et al. Second-order consensus for nonlinear leader-following multi-agent systems via dynamic output feedback control. International Journal of Robust and Nonlinear Control, 2016, 26(2): 329 – 344.

[9] YU J L, DONG X W, LI Q D, et al. Distributed time-varying formation control for second-order nonlinear multi-agent systems based on observers. Proc. of the Control & Decision Conference, 2017: 6313 – 6318.

[10] MEI J, REN W, MA G. Distributed coordination for second-order multi-agent systems with nonlinear dynamics using only relative position measurements. Automatica, 2013, 49(5): 1419 – 1427.

[11] MEI J, REN W, CHEN J. Distributed consensus of second-order multi-agent systems with heterogeneous unknown inertias and control gains under a directed graph. IEEE Trans. on Automatic Control, 2016, 61(8): 2019 – 2034.

[12] DONG X W, HAN L, LI Q D, et al. Time-varying formation control for double-integrator multi-agent systems with jointly connected topologies. International Journal of Systems Science, 2016, 47(16): 3829 – 3838.

[13] LU X Q, AUSTIN F, CHEN S H. Formation control for second-order multi-agent systems with time-varying delays under directed topology. Communications in Nonlinear Science and Numerical Simulation, 2012, 17(3): 1382 – 1391.

[14] HUANG N, DUAN Z S, CHEN G R. Some necessary and sufficient conditions for consensus of second-order multi-agent systems with sampled position data. Automatica, 2016, 63: 148 – 155.

[15] DONG X W, ZHOU Y, REN Z, et al. Time-varying formation tracking for second-order multi-agent systems subjected to switching topologies with application to quadrotor formation flying. IEEE Trans. on Industrial Electronics, 2017, 64(6): 5014 – 5024.

[16] DONG X W, HAN L, LI Q D, et al. Time-varying formation tracking for second-order multi-agent systems with one leader. Proc. of the Chinese Automation Congress, 2015: 1046 – 1051.

[17] DONG X W, HU G Q. Time-varying formation tracking for linear multiagent systems with multiple leaders. IEEE Trans. on Automatic Control, 2017, 62(7): 3658 – 3664.

[18] HAN L, DONG X W, LI Q D, et al. Formation tracking control for second-order multi-agent systems with time-varying delays. Proc. of the 35th Chinese Control Conference, 2016: 7902 – 7907.

[19] HAN L, DONG X W, LI Q D, et al. Formation tracking control for time-delayed multi-agent systems with second-order dynamics. Chinese Journal of Aeronautics, 2017, 30(1): 348 – 357.

[20] LIU M, WANG Y W, XIAO J W, et al. Formation tracking

control for multi-agent systems with nonlinear dynamics via impulsive control. Proc. of the Control and Decision Conference, 2014: 3669 – 3674.
[21] ZHAO Q L, DONG X W, LIANG Z X, et al. Distributed group cooperative guidance for multiple missiles with switching directed communication topologies. Proc. of the 36th Chinese Control Conference, 2017: 5741 – 5746.
[22] SUN H B, LI S H, SUN C Y. Robust adaptive integral-sliding-mode fault-tolerant control for airbreathing hypersonic vehicle. Journal of Systems and Control Engineering, 2012, 226(10): 1344 – 1354.
[23] GAO Z F, JIANG B, SHI P, et al. Passive fault-tolerant control design for near-space hypersonic vehicle dynamical system. Circuits, Systems, and Signal Processing, 2012, 31(2): 565 – 581.
[24] QI R, HUANG Y, JIANG B, et al. Adaptive backstepping control for a hypersonic vehicle with uncertain parameters and actuator faults. Journal of Systems and Control Engineering, 2012, 227(1): 51 – 61.
[25] WANG Y, SONG Y D, LEWIS F L. Robust adaptive fault-tolerant control of multiagent systems with uncertain nonidentical dynamics and undetectable actuation failures. IEEE Trans. on Industrial Electronics, 2015, 62(6): 3978 – 3988.
[26] HUA Y Z, DONG X W, LI Q D, et al. Fault-tolerant time-varying formation control for second-order multi-agent systems with directed topologies. Proc. of the IEEE International Conference on Control& Automation, 2017: 467 – 472.
[27] WANG Y J, SONG Y D, KRSTIC M, et al. Fault-tolerant finite time consensus for multiple uncertain nonlinear mechanical systems under single-way directed communication interactions and actuation failures. Automatica, 2016, 63: 374 – 383.
[28] SALIMIFARD M, ALI TALEBI H. Robust output feedback fault-tolerant control of non-linear multi-agent systems based on wavelet neural networks. Control Theory & Applications, 2017, 11(17): 3004 – 3015.
[29] NGUYEN M T, STOICA MANIU C, OLARU S, et al. Fault tolerant predictive control for multi-agent dynamical: formation reconfiguration using set-theoretic approach. Proc. of the IEEE International Conference on Control, Decision and Information Technologies, 2014: 417 – 422.
[30] KHALILI M, ZHANG X D, CAO Y C, et al. Distributed adaptive fault-tolerant consensus control of multi-agent systems with actuator faults. Proc. of the Annual Conference of the Prognostics and Health Management Society, 2015: 1 – 8.
[31] GUO J Y, LIU X F, JIANG C X, et al. Distributed fault-tolerant topology control in cooperative wireless ad hoc networks. IEEE Trans. on Parallel and Distributed Systems, 2015, 26(10): 2699 – 2710.
[32] JEON I S, LEE J I, TAHK M J. Homing guidance law for simultaneous attack of multiple missiles. Journal of Guidance Control and Dynamics, 2010, 33(1): 275 – 280.
[33] SALEEM A, RATNOO A. Lyapunov-based guidance law for impact time control. Journal of Guidance Control and Dynamics, 2016, 39(1): 164 – 173.
[34] ERER K S, TEKIN R. Impact time and angle control based on constrained optimal solutions. Journal of Guidance Control and Dynamics, 2016, 39(10): 2445 – 2451.
[35] CHO D, KIM H J, TAHK M J. Nonsingular sliding mode guidance for impact time control. Journal of Guidance Control and Dynamics, 2016, 39(1): 61 – 68.
[36] CRAIG R E, REICH R J. Flight test aerodynamic drag characteristics development and assessment of in-flight propulsion analysis methods for the AGM-109 cruise missile. Proc. of the AIAA Flight Test Conference, 1981: AIAA 1981 – 2423.
[37] MCGRATH B. Subsonic aerodynamic fin-folding moments for the tactical tomahawk missile configuration. Proc. of the AIAA 22nd Applied Aerodynamics Conference and Exhibit, 2004: AIAA 2004 – 5193.
[38] NEWMAN A M, ROSENTHAL R E, SALMERÓN J, et al. Optimizing assignment of Tomahawk cruise missile missions to firing units. Naval Research Logistics, 2011, 58(3): 281 – 294.
[39] XU X G, WEI Z Y, REN Z, et al. Fault-tolerant time-varying formation tracking for second-order multi-agent systems subjected to directed topologies and actuator failures with application to cruise missiles. Proc. of the Chinese Intelligent Systems Conference, 2018: 845 – 861.
[40] LEONG P H, ARULAMPALAM S, LAMAHEWA T A, et al. A Gaussian-sum based cubature Kalman filter for bearings-only trackin. IEEE Trans. on Aerospace and Electronic Systems, 2013, 49(2): 1161 – 1176.
[41] NGAI M K, HA Q P, HUANG S D, et al. Mobile robot localization and mapping using a Gaussian sum filter. International Journal of Control, Automation, and Systems, 2007, 5(3): 251 – 268.
[42] HAN J Q. Active disturbance rejection control technique-the technique for estimating and compensating the uncertainties. Beijing: National Defense Industry Press, 2008: 197 – 210. (in Chinese)

Biographies

XU Xingguang was born in 1988. He received his B.E. degree from Northwestern Polytechnical University in 2007 and M.S. degree from the Third Institute of China Aerospace Science and Industry Corporation Limited in 2014. He is now a Ph.D. candidate in navigation, guidance and control in Beihang University and also an engineer in Beijing Institute of Mechanical and Electrical Engineering. His research interests include aircraft design, fault-tolerant control, and cooperative control of multi-agent systems.
E-mail: xuxingguang@buaa.edu.cn

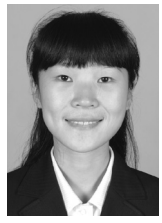

WEI Zhenyan was born in 1983. She received her B.E. degree from Harbin Institute of technology in 2006 and M.S. degree from the Third Institute of China Aerospace Science and Industry Corporation Limited in 2009. She is now a Ph.D. candidate in navigation, guidance and control in Beihang University and also a professor in Beijing Aerospace Technology Institute. Her research interests include aircraft control and adaptive control.
E-mail: weizhenyan@buaa.edu.cn

REN Zhang received his B.E., M.E. and Ph.D. degrees in aircraft guidance, navigation, and simulation from Northwestern Polytechnical University in 1982, 1985 and 1994, respectively. He held the visiting professor position with University of California, Riverside, and Louisiana State University, USA, respectively. He is now a professor with the School of Automation Science and Electronic Engineering, Beihang University. His research interests include aircraft guidance, navigation and control, fault detection, isolation and recovery and cooperative control of multi-agent systems.
E-mail: renzhang@buaa.edu.cn

LI Shusheng was born in 1962. He is now a professor and Ph.D. supervisor in the Third Institute of China Aerospace Science and Industry Corporation Limited. He is a national outstanding contribution expert in the field of tracks and controls and is granted a Special Allowance from the State Council. His research interests include aircraft design, fault diagnosis, tracks and controls and design for testability.
E-mail: dpnyjxxg521@163.com